X-932-75-47

PREPRINT

ON THE NATURE OF THE RADIAL AND CROSS TRACK ERRORS FOR ARTIFICIAL EARTH SATELLITES

N. L. BONAVITO
R. A. GORDON
J. G. MARSH

MARCH 1975

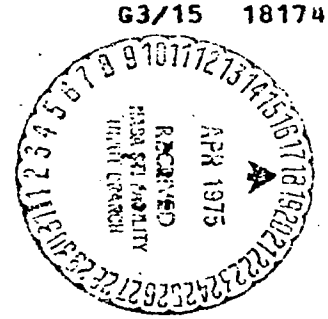

GODDARD SPACE FLIGHT CENTER
GREENBELT, MARYLAND

X-932-75-47

ON THE NATURE OF THE RADIAL AND CROSS TRACK ERRORS FOR ARTIFICIAL EARTH SATELLITES

N. L. Bonavito
R. V. Gordon
J. G. Marsh

March 1975

GODDARD SPACE FLIGHT CENTER
Greenbelt, Maryland

CONTENTS

LIST OF ILLUSTRATIONS

ON THE NATURE OF THE RADIAL AND CROSS TRACK ERRORS FOR ARTIFICIAL EARTH SATELLITES

N. L. Bonavito
R. A. Gordon
J. G. Marsh

ABSTRACT

In this paper we discuss the analysis of the radial and cross track errors of artificial Earth satellites in terms of the interference of two one dimensional celestial mechanical wave trains. The resulting equations for these tracking errors describe the behavior of the uncertainties in the orbital parameters as oscillatory in nature, with a rapidly oscillating term, which is a function of the sum of the observed and computed orbital frequencies, modulated in amplitude by a slowly varying oscillation. This latter term is itself a function of either the difference between these orbital frequencies or between the values of the computed and observed right ascensions, depending upon whether it is the radial or cross track case under consideration. In theoretical physics, this effect is referred to as the phenomenon of beats and is common in the physics of sound and elastic media. These results indicate that the cross track calculation describes the behavior of uncertainties in the right ascension of the ascending node and the inclination, while the radial calculation gives information on uncertainties in

the semi-major axis, the eccentricity, and the argument of perigee. Analysis is done for the U. S, Air Force Cannonball (OAR-901) and GEOS-II satellites.

In addition, expressions for the radial and cross track oscillatory frequencies are obtained in terms of the orbital frequencies of the satellites. These oscillatory frequencies are functions only of the zonal harmonic terms of the Earth's gravitational potential, and are used to analyze the behavior of the tracking errors in terms of uncertainties in the gravitational field coefficients.

Finally, we show that the time average of the radial and cross track errors in any case, will both approach zero.

I. INTRODUCTION

There has been considerable interest in the error analysis of spacecraft trajectory systems. Error analysis can be defined as the ability to describe the effect of inherent uncertainties of an overall orbital determination system on the computational accuracy of the system. There are several sources responsible for the presence of such uncertainties, with perhaps the most important due to the inability to correctly describe the physics of the problem. As a result, the physical data that is used, and the modelling of the forces involved, provide at best, only a good starting point for the calculation of an orbit. The accuracy of the observational data will depend upon the type and quality of the tracking technique that is employed. Even after fitting an orbit, the post convergence residuals do not account for uncertainties in coordinates of the tracking sites. More important, even though the constants of integration may be well determined, the accuracy of the calculated orbit will still depend upon the accuracy of the differential equations of motion. In any event, the overall uncertainty in the calculated coordinates of a spacecraft can be defined within the framework of a time dependent error bound (Reference 1). One method of studying the effect of uncertainties in orbit determination is to examine the radial and cross track errors. The cross track error is defined as the difference at any instant of time, between the position vectors of an observed and calculated, or two calculated orbits, projected in the direction of the unit angular momentum vector of one of these systems, provided that both systems are conservative ones. In

addition, the radial error is defined as this same difference projected along the instantaneous unit radius vector of one of the orbits. If the orbit system can be considered as a conservative one, then calculation of the radial and cross-track errors can be used to study errors produced by various gravity models. Such results are of considerable importance in the field of geodesy.

In this paper we shall review these concepts in the light of classical theoretical physics and compare the results with real and simulated data of various orbit systems.

II. STATEMENT OF THE PROBLEM

Let us now define an inertial coordinate system, fixed at the Earth's center with the x-axis pointing toward Aries, z through the geographic North Pole, and y set so as to form a righthanded system. Then the observed position vector of a point mass in orbit is given by $\vec{r}_0 = \vec{i}\, x_0 + \vec{j}\, y_0 + \vec{k}\, z_0$, where $\vec{i}$, $\vec{j}$ and $\vec{k}$ are the orthogonal unit vector set. The observed velocity is given by $\vec{v}_0 = \vec{i}\, v_x + \vec{j} v_y + \vec{k}\, v_z$, and the computed values of these quantities are designated as $\vec{r}_c = \vec{i}\, x_c + \vec{j}\, y_c + \vec{k}\, z_c$, and $\vec{v}_c = \vec{i}\, v_{x_c} + \vec{j} v_{y_c} + \vec{k} v_{z_c}$ respectively. From the above discussion we then have that the cross track error

$$N = \frac{\vec{L}_0}{|\vec{L}_0|} \cdot \Delta\vec{r} \tag{1}$$

where $\vec{L}_0 = (\vec{r}_0 \times \vec{v}_0)$, and $\Delta\vec{r} = (\vec{r}_0 - \vec{r}_c)$. The radial error is given by

$$R = \frac{\vec{r}_0}{|\vec{r}_0|} \cdot \Delta\vec{r} \tag{2}$$

Before proceeding with a theoretical analysis, let us briefly examine these two equations. If we assume that our system is a conservative one, that is, if there are no forces present drawing energy from the orbit, then we have that the Hamiltonian, namely, the kinetic plus potential energy, is the total energy. In addition, if time is not explicitly present, then the Hamiltonian is also a constant of the motion Furthermore, the total angular momentum and the z-component of angular momentum are constants of the motion. Now the gravitational potential energy can be written as a generalized solution of Laplace's equation, namely,

$$V = \frac{\mu}{r}\left[1 + \sum_{n=1}^{\infty}\sum_{m=0}^{n}\left(\frac{r_e}{r}\right)^n P_n^m(\cos\theta)\,(C_{n,m}\cos m\lambda + S_{n,m}\sin m\lambda)\right]$$

where μ is the product of the gravitational constant and the planet's mass, r_e is its equatorial radius, r and θ are the planetocentric distance and colatitude of a field point, $C_{n,m}$ and $S_{n,m}$ are the coefficients of potential, λ is the angle of east longitude, and $P_n^m(\cos\theta)$ are the associated Legendre functions. In practice, one tries to include all forces in nature acting on the system in the Hamiltonian, and in the process of orbit determination, a complete knowledge of the geodetic constants and coefficients of the Earth's gravitational potential is necessary for perfect orbit calculation. Since such information is not available, and in addition, since present computational techniques are insufficient to maintain agreement with observation for more than a few days, then it is customary to compensate for these errors by reinitializing the constants of integration through a fitting procedure by comparing theory with observation over an arc of

several days. However, it appears that there may be a limitation to what we may know about the gravitational field. For example, the possibility of mass transport in the liquid outer core of the Earth, even if uniform, would still give rise to density fluctuations. In addition, mass transport arising from rapid first order phase transitions (condensation of matter under enormous pressure) within the lithosphere could create local density changes which would correspond to a creation and destruction of higher order coefficients in the gravity field. More advanced theories indicate that rapid first order polymorphic phase transitions may be the source of deep focus earthquakes, manifesting as irregularities or breaks in the Chandler wobble of the Earth. It is also estimated that during such an event, enough mass is shifted so as to cause as much as a 0.1 to 0.4 milligal change in the local value of gravity. In any event, such considerations seem to place a temporary if not permanent restriction on a complete theoretical description of the gravitational field and the subsequent accuracy of the predicted positions of a spacecraft.

In spite of such limitations however, we can still make the following rationalizations: Since the total energy, and the angular momentum are constants of the motion, then the energy difference of the computed and observed orbits which is manifest through the spacecraft radius vector by way of the semi-major axis, is a bound quantity. As a consequence, one might expect the radial error to be bound, and since the angular momentum is conserved, the cross-track would be likewise.

III. INTERFERENCE OF WAVES

The problem that now suggests itself from the above discussion, is the nature of the tracking errors arising from an inability to properly or adequately specify the potential energy through the coefficients of the gravitational field. In actual practice, tracking errors are often calculated by one of the following methods: For a given potential energy, two partially overlapping arcs of fitted data are obtained on a spacecraft by comparing observations of position and velocity with those calculated using the given potential. The positions and velocities in each of the overlapping portions of the fitted arcs corresponding to a particular time are then used in equations (1) and (2) to determine the cross and radial track errors. In this case, the potential is fixed, and the coordinates (within the fitted arcs) are changed. In the other case, positions and velocities of two slightly different orbits are compared at corresponding times, and the tracking errors are again computed for each of these times. Here the initial conditions and the equations of motion are the same, but values of the coefficients of the Earth's gravitational potential differ slightly for each orbit.

Technically speaking, interference is a term referring to the physical effects of superimposing two or more wave trains. As in the case of elastic media, it is desirable to define a 'wave equation' which contains information on the behavior of the system. We now consider the polar equation of an ellipse,

$$r = a(1 - e \cos E) \tag{3}$$

where a, e, and E are the semi-major axis, eccentricity, and eccentric anomaly respectively. A one dimensional representation of this equation is obtained by multiplying by the cosine of the true anomaly. Therefore,

$$y = r \cos \nu = a(1 - e \cos E) \cos \nu, \tag{4}$$

and using the anomaly connection for the true and eccentric anomaly,

$$\cos \nu = \frac{(\cos E - e)}{1 - e \cos E}, \tag{5}$$

$$y = a \cos E - ae. \tag{6}$$

This is our one-dimensional wave equation for elliptic motion of an artificial satellite, referenced to the major axis of the ellipse.

Let us now consider two waves of equal frequency and amplitude travelling with the same speed in the same direction, but with a phase difference ϕ between them. Therefore, with the conditions that $a_1 = a_2 = a$, $e_1 \neq e_2$, and $E = 2\pi ft$, we have for the two waves

$$y_1 = a \cos(2\pi f_1 t) - ae_1 \tag{7}$$

$$y_2 = a \cos(2\pi f_1 t - \phi) - ae_2. \tag{8}$$

The resultant wave which is the difference of equations (7) and (8) is,

$$y = y_1 - y_2 = (ae_2 - ae_1) - a[\cos(2\pi f_1 t) - \cos(2\pi f_1 t - \phi)].$$

From the trigonometric equation for the difference of the cosines of two angles,

$$\cos A - \cos B = -2 \sin \frac{1}{2}(A + B) \cdot \sin \frac{1}{2}(A - B). \tag{9}$$

we obtain,

$$y = a(e_2 - e_1) - \left[2a \sin \frac{\phi}{2}\right] \sin 2\pi \left(f_1 t - \frac{\phi}{2}\right) \tag{10}$$

This resultant wave corresponds to a new wave having the same frequency f_1 but with an amplitude, $2a \cdot \sin \phi/2$. If ϕ is very small, the resultant amplitude will be nearly zero. As a result, equation (10) suggests that the radial tracking error as given by equation (2) will oscillate with the same frequency as the orbital frequency but with amplitude determined by any phase difference between the computed and observed orbits. A phase difference in the eccentric anomaly however, is equivalent to one in both the true and the mean anomaly also. Since the orbital periods are the same here, then a phase difference between the two eccentric anomalies arises for example from a poor determination of the argument of perigee. Near the beginning of the orbit therefore, this uncertainty in the argument of perigee will be a factor in the magnitude of the rapid oscillatory term of equation (10).

Let us now consider the case of two wavetrains similar to the above, but with slightly different frequencies, travelling through the same region. The two displacements can be represented as

$$y_1 = a \cos 2\pi f_1 t - ae_1, \tag{11}$$

and

$$y_2 = a \cos(2\pi f_2 t - \phi) - ae_2. \tag{12}$$

The difference is

$$y = y_1 - y_2 = a(e_2 - e_1) - 2a \sin \left[2\pi \left(\frac{f_1 - f_2}{2}\right) t + \frac{\phi}{2}\right] \cdot \sin \left[2\pi\left(\frac{f_1 + f_2}{2}\right) t - \frac{\phi}{2}\right]. \tag{13}$$

The resulting vibration may then be considered to have a frequency

$$\overline{f} = \frac{f_1 + f_2}{2}$$

which is the average of the two waves, and an amplitude given by the expression in the brackets. Therefore, the amplitude varies with time with a frequency:

$$\delta = \frac{f_1 - f_2}{2}.$$

If f_1 and f_2 are nearly equal, this term is small and the amplitude fluctuates slowly. This phenomenon is a form of amplitude modulation and is commonly referred to as 'beats'. A beat, or a maximum of amplitude will occur whenever

$$\sin 2\pi \left[\left(\frac{f_1 - f_2}{2}\right) t + \frac{\phi}{2}\right]$$

equals 1 or -1. In orbital motion, the frequency of rotation is governed primarily by the value of t' : semi-major axis. This demands that y_1 and y_2 of equations (11) and (12) contain different values of a, which would result in a numerical determination of $y_1 - y_2$ versus time. However, since amplitudes only add together algebraically, the general behavior of the system is still described analytically by equation (13). The interference of two waves of different amplitudes, frequencies, and phases, would ordinarily result in a distorted complex waveform, but the analysis of equations (1) and (2) can be made more directly through equations (10) and (13). Equation (13) implies that errors in the computed value of the semi-major axis, and to a lesser degree, the ·centricity and argument of perigee determine both the amplitude and the frequency of the envelope of the radial tracking error (Figure 1). Equation (10) indicates that any distortion in the envelope is due to a timing error in the mean anomaly. If the semi-major axes of the two systems under comparisons are almost equal initially, then the corresponding frequencies or periods are likewise almost identical. Because of this, the advance of perihelion for each orbit is approximately the same, and the angular difference between each perigee (or apogee) increases slowly. When this difference is π, the respective apogees are exactly out of phase, and the magnitude of their difference is at its maximum. This is also the maximum of the amplitude of equation (13). If the periods are long, and in addition, if they are close in value, then the time between succeeding maxima may be very large. Figure 2 shows a plot of the radial error versus time for the cannonball

(OAR-901) satellite (a = 8335.34 km, e = 0.123, and i = 92.00 degrees). The graph was generated using the Brouwer theory of artificial satellite motion (Reference 2). For the calculation, the potentials used only the first two zonal harmonics, with the second zonal coefficients given by $J_2 = -1.0825 \times 10^{-3}$ and $J_2' = 0.90 \times J_2$. In this case, the period between maxima (or minima) is approximately 120 days (Figure 2). The value of the eccentricity determines the symmetry character of the oscillation. If e is much different from zero, then Kepler's law demands that the spacecraft spend more time near apogee. When the two orbits are essentially coincidental, the positional differences are smallest. As the angle between the major axes increases, these differences increase, and the maximum is obtained when this angle is π, and as described above, when the spacecraft are at their respective apogee points. Between π and 2π, the position differences decrease, becoming a minimum at 2π. If the reference orbit is 'larger' that is, if the semi-major axis of the reference orbit is larger than that of the 'computed' orbit, then radial error will 'arc' positively. As the angle between the positional differences, in the plane of the reference orbit increases, the magnitude of their difference will also increase, and the envelope of equation (13), given by

$$\left[2a \sin 2\pi\left(\frac{f_1 - f_2}{2}\right) t + \frac{\varphi}{2}\right]$$

will also reach its maximum value given by twice the semi-major axis. The time for this to occur will depend on the value of $f_1 - f_2$. In Figure 2, the

maximum of the variation is approximately 16,000 km. The constant term $a(e_2 - e_1)$ also represents a shift about which the radial error oscillates.

We can now summarize briefly. A comparison of a plot of equation (2) and equation (13), shows the following: An 'error' or uncertainty in the eccentricity will appear as a shift along the ordinate axis, about which an oscillation in time of the radial error occurs. This oscillation is of frequency $(f_1 + f_2)/2$ where f_1 and f_2 represent a computed and observed orbital frequency. This rapid oscillation which is close to both f_1 and f_2 is then modulated by a much lower frequency oscillation of value $(f_1 - f_2)/2$, and with amplitude 2a. The frequency of the orbit varies inversely as the period, and the period is a function of the semi-major axis. As a result, a difference between the computed and observed values of the semi-major axes results in a finite value of $f_1 - f_2$, and a slow modulation of the rapid radial oscillation appears. The result suggests a beat phenomena, common in the theory of sound. The beat frequency is given by $(f_1 - f_2)/2$, and as f_1 approaches f_2, that is, as the difference between the computed and observed values of the semi-major axes approaches zero, the period of the beat phenomena becomes large.

We now turn to the discussion of the nature of the cross track error given by equation (1). Let us assume that at the initial time, the six orbital parameters which describe the computed system differ slightly from those of the observed orbit. At some later time, we also assume that the component of the positior vector of the spacecraft from the observed orbit into

the corresponding line of nodes is $r_2 \cos u_2$, where $r_2 = a_2(1 - e_2 \cos E_2)$, $u_2 = \omega_2 + \nu_2$, ω_2 is the argument of perigee, and ν_2 is the true anomaly. For the computed orbit, we have similarly, $r_1 \cos u_1$ along its line of nodes. The wave trains, represented by $r_2 \cos u_2$ and $r_1 \cos u_1$ need to be referenced to a common axis to discuss interference effects. However, for the cross-track error component, we need the perpendicular component of the observation on the calculated orbit, and hence, we wish to have the two wave trains interfere with each other but at right angles. Physically, this is the same as sighting parallel to the $r_1 \cos u_1$ wave, and observing the oscillatory behavior of the $r_2 \cos u_2$ wave with respect to the first. Therefore, the projection of $r_2 \cos u_2$ onto the line of nodes of the computed orbit is given by $r_2 \cos u_2 \cdot \sin(\Omega_2 - \Omega_1)$, where Ω_2 and Ω_1 are the respective right ascensions of the ascending node for each orbit. Since the observed system is inclined at an angle i_2, the projection is not perpendicular to the computed orbit. The perpendicular component is obtained by a rotation through this inclination. The result is

$$y_\Omega = a_2 \sin i_2 \cdot \sin(\Omega_2 - \Omega_1) [\cos \omega_2 \cdot \cos E_2 - \sqrt{1 - e_2^2} \sin \omega_2 \cdot \sin E_2 - e_2 \cos \omega_2]. \quad (14)$$

However, since the observed and computed orbits are not parallel, there is another contribution to the cross-track term originating from the discrepancy in the inclinations. Results show that both this term and its variation are very small. Nevertheless, its contribution is,

$$y_i = r_2 \sin(i_2 - i_1) = a_2(1 - e_2 \cos E_2) \sin(i_2 - i_1). \tag{15}$$

The sum of (14) and (15) give the result we want, namely,

$$y = y_\Omega + y_i = a_2 \sin i_2 \cdot \sin(\Omega_2 - \Omega_1) \left[\cos \omega_2 \cdot \cos E_2 - \sqrt{1 - e_2^2} \sin \omega_2 \cdot \sin E_2 - e_2 \cos \omega_2\right] + a_2(1 - e_2 \cos E_2) \sin(i_2 - i_1). \tag{16}$$

If e is sufficiently small, we have,

$$y = a_2 [\sin i_2 \cdot \sin(\Omega_2 - \Omega_1) \cdot \cos(E_2 + \omega_2) + \sin(i_2 - i_1)]. \tag{17}$$

The angular velocity of the eccentric anomaly is much greater than that of the argument of perigee (usually two orders of magnitude), so that the cross-track error displays a rapid oscillation with a frequency approximately that of the orbital frequency, modulated by a slowly increasing sinusoidal function with maximum amplitude $a_2 \sin i_2$. This is again analogous to beat phenomena, and the respective maxima are obtained when the two orbit systems differ in their values of the ascending node by $\pi/2$. Figure 3 shows a plot of the cross-track error for the Cannonball satellite using the above values of J_2 and J_2'. The beat period or that period between successive minima (or maxima) is seen to be approximately 870 days for this case. Equations (16) and (17) suggest that as the values of the computed and observed right ascensions become more in agreement, the beat period becomes progressively larger, with a maximum

amplitude of a sin i. In our example, i = 92°, so that sin i ≃ 1, and the maximum theoretical cross track amplitude according to equations (16) and (17) is approximately 8000 km, which is in close agreement to that given by equation (1).

Figures 4 and 5 illustrate the use of equations (1) and (2) in the determination of the cross and radial tracking error for a small portion of the orbit of the GEOS-II satellite (a = 7700.00 km, e = 0.032, and i = 105.80 degrees). The tracking data consisted of Navy Tranet Doppler observations recorded by a globally distributed set of tracking stations. The orbits were computed using the GSFC GEM-1 (Reference 3) and the SAO 1969 (Reference 4) Standard Earth gravity models. Perturbations due to solar-lunar gravity, direct solar radiation pressure, and air drag were also modelled in the solutions, so that the primary error source is the Earth's gravity field. The orbital solutions were obtained using the GEODYN orbit and geodetic parameter estimation system. For both the GSFC GEM-1 and SAO 1969 cases, orbital arc lengths of two days were used covering the periods 12 hours, 15 minutes of May 23, 1968 to 12 hours, 15 minutes of May 25, 1968, and 12 hours, 15 minutes of May 24, 1968 to 12 hours, 15 minutes of May 26, 1968. The cross and radial tracking errors were determined during the one day overlap from 12 hours, 15 minutes of May 24, 1968 to 12 hours, 15 minutes of May 25, 1968. Because of the short period over which the calculations were performed, the periods of the beat phenomena for both the radial and cross track terms are not shown. According to equations (13) and (17), the corresponding maxima are 15,400 km and 7700 km respectively for these

fitted arcs. An examination of the radial error for the GEM-1 case shows a slowly increasing envelope, but with a downward drift, indicating that the computed value of the semi-major axis is larger than the observed value. To determine this latter value, we would proceed in the following manner: The radial oscillatory period, $\bar{P}$ is read off of the graph (Figure 4 or 5). From this,

$$\bar{f} = \frac{f_0 + f_c}{2} = \frac{1}{\bar{P}}. \tag{18}$$

Using the fitted data for this arc, the computed period f_c is calculated by

$$\Gamma_c = 2\pi\mu^{-1/2} a^{3/2} \tag{19}$$

where a is obtained from the orbit improvement process. Therefore $f_c = 1/P_c$. The observed frequency f_0 is then given by

$$f_0 = 2\bar{f} - f_c, \tag{20}$$

and from this,

$$P_0 = \frac{1}{f_0}, \tag{21}$$

From the expression for the period such as equation (19), the observed value of the semi-major axis is obtained. The difference between this and the fitted value of the semi-major axis gives us the discrepancy in the latter. Figures 4 and 5 are not sufficiently expanded to give accurate values of $\bar{P}$ and a $(e_2 - e_1)$. The magnitudes of the radial errors for these two graphs indicate a slightly more serious phasing problem or uncertainty in the argument of perigee for the

Standard Earth solution. On the other hand, the slope of the radial envelopes suggests that the Standard Earth value of the semi-major axis may be closer to the observed value than that of GEM-1. This could be resolved by a calculation such as given above.

For the cross track component, the time scale of figures 4 and 5 are too short to make an accurate estimate of the discrepancy in the right ascension of the ascending node for the Standard Earth and the GEM-1 cases, as described by equation (17).

In this section, we have attempted to reduce the analysis of the cross and radial tracking errors given by equations (1) and (2) above, to an analysis of the resultant behavior of the interference of two one-dimensional 'celestial mechanical wave trains'. These results, namely equations (13) and (17), then describe the behavior of, and the discrepancies between, the computed and observed values of the orbital parameters for a given potential or gravitational field for any arc of the orbit. The radial wave equation gives information on the semi-major axis, the eccentricity and to a limited extent, the argument of perigee. The cross track wave equation gives information on the right ascension of the ascending node and the inclination. Thus, five of the six orbital parameters are examined by this procedure. This leaves only the mean anomaly. To accurately assess its behavior and any discrepancy between the observed and computed value of this parameter, it is necessary to make a careful analysis of the corresponding in-track error component. From Kepler's law, it is obvious that for different

values of the sidereal mean motion, two orbits will sweep out different equal areas and different values of the true anomaly in equal times. From the anomaly connections between the true and eccentric anomaly and using Kepler's law, the mean anomaly,

$$M = E - e \sin E, \tag{22}$$

will vary accordingly.

IV. FREQUENCY EQUATIONS

In the previous section we discussed the analysis of the tracking errors by relating their behavior to uncertainties in the orbital parameters. By this approach, we wish to ascertain the degree to which these orbital parameters are involved in the accuracy of the trajectory calculation. In this section however, we attempt to relate the behavior of the radial and cross track errors to certain of the coefficients of the Earth's gravitational field. As a result, some information can be derived from the relationship between these orbital parameters and the values of gravitational coefficients used in the calculations.

As a starting point for our calculation, let us consider the following expression for the gravitational potential $V(r, \theta)$, written in terms of an expansion in spherical harmonics:

$$V = \frac{\mu}{r}\left[1 + \sum_{n=1}^{\infty} J_n \left(\frac{r_e}{r}\right)^n P_n(\cos\theta)\right]. \tag{23}$$

In addition, we also consider the following problem: A spacecraft represented by a point mass moves in orbit about a planet whose gravitational potential is given by equation (23). At some time which we shall take to be the epoch of the orbit, an instantaneously small but finite impulse is applied to the point mass. The problem is to describe the subsequent motion. We note that the impulse has the effect of disturbing the coordinates of the satellite at this initial or epoch time, while the potential field is constant. The Hamiltonian for this system, which is also the total energy, can be written as

$$\mathcal{H} = E = \frac{1}{2} m\dot{r}^2 + \frac{1}{2} mr^2\dot{\theta}^2 + \frac{1}{2} mr^2 \sin^2\theta\dot{\phi}^2 + V(r, \theta). \tag{24}$$

Here, the geocentric right ascension ϕ is cyclic, and as a result, its canonically conjugate momentum

$$p_\phi = mr^2 \sin^2\theta\dot{\phi} = \text{constant}. \tag{25}$$

We may introduce an effective potential $'V'(r, \theta)$ for the motion:

$$'V'(r, \theta) = V(r, \theta) + \frac{p_\phi^2}{2mr^2 \sin^2\theta}. \tag{26}$$

If we now assume that the colatitude coordinate is held fixed, and there is a small change in r only, then we have from equation (24),

$$E - 'V'(r) = \frac{1}{2} m\dot{r}^2. \tag{27}$$

Since the right hand member cannot be negative, the motion must be confined to those values of r for which $'V'(r) \leq E$. The relationship between p_ϕ and the equilibrium radius $r_\mathcal{E}$, that is, the radius prior to the applied impulse is,

$$\left[\frac{d\,'V'(r)}{dr}\right]_{r_\mathcal{E}} = \left(\frac{dV(r)}{dr}\right)_{r_\mathcal{E}} - \frac{p_\phi^2}{m r_\mathcal{E}^3 \sin^2\theta} = 0. \tag{28}$$

Combining equations (28) and (25) we have,

$$\dot{\phi}_r^2 = \left(\frac{dV(r)}{dr}\right)_{r_\mathcal{E}} \frac{1}{m r_\mathcal{E} \sin^2\theta}. \tag{29}$$

From equations (24) and (28) the equilibrium energy is

$$E_\mathcal{E} = \frac{r_\mathcal{E}}{2}\left(\frac{dV(r)}{dr}\right)_{r_\mathcal{E}} + V(r_\mathcal{E}) + \frac{1}{2} m \dot{r}_\mathcal{E}^2 \tag{30}$$

For an energy slightly larger than $E_\mathcal{E}$, and an angular momentum p_ϕ given by equation (28), the coordinate r will perform simple harmonic oscillations about the value $r_\mathcal{E}$. If we set

$$k_r = \left[\frac{d^2\,'V'(r)}{dr^2}\right]_{r_\mathcal{E}} = \left(\frac{d^2V(r)}{dr^2}\right)_{r_\mathcal{E}} + \frac{3p_\phi^2}{m r_\mathcal{E}^4 \sin^2\theta}, \tag{31}$$

Then for small values of $(r - r_\mathcal{E})$, we can expand $'V'(r)$ in a Taylor series:

$$'V'(r) = E_\mathcal{E} + \frac{1}{2} k_r (r - r_\mathcal{E})^2. \tag{32}$$

The energy equation (27), now becomes

$$E - E_{\mathcal{E}} = \frac{1}{2} m\dot{r}^2 + \frac{1}{2} k_r (r - r_{\mathcal{E}})^2 \tag{33}$$

This is the energy for a harmonic oscillator with energy $(E - E_{\mathcal{E}})$, coordinate $(r - r_{\mathcal{E}})$, mass m, and spring constant k_r. Then for a small impulse, the radial component of the radius vector will oscillate about the equilibrium value $r_{\mathcal{E}}$ with a frequency given by,

$$\omega_r^2 = \frac{k_r}{m} = \left[\frac{1}{m}\left(\frac{d^2V(r)}{dr^2}\right)_{r_{\mathcal{E}}} + \frac{3p_\phi^2}{m^2 r_{\mathcal{E}}^4 \sin^2\theta}\right]. \tag{34}$$

It is of interest to compare ω_r^2 and $\dot{t}_r^2$: From (29) and (34) we have,

$$\omega_r = \left\{\left[\frac{1}{m}\left(\frac{d^2V(r)}{dr^2}\right)_{r_{\mathcal{E}}} + \frac{3p_\phi^2}{m^2 r_{\mathcal{E}}^4 \sin^2\theta}\right] mr_{\mathcal{E}} \sin^2\theta \Big/ \left(\frac{dV(r)}{dr}\right)_{r_{\mathcal{E}}}\right\}^{1/2} \dot{\phi}_{r_{\mathcal{E}}}. \tag{35}$$

In other words, we now have the frequency of oscillation of the perturbed radial component of the radius vector in terms of the undisturbed or equilibrium value of the orbital period as given by the motion of the geocentric right ascension, and the first and second derivatives of the gravitational potential energy. A similar argument for the colatitude angle θ, yields the harmonic oscillator energy equation,

$$E - E_{\mathcal{E}} = \frac{1}{2} mr^2\dot{\theta}^2 + \frac{1}{2} k(\theta - \theta_{\mathcal{E}})^2, \tag{36}$$

with energy $(E - E_{\mathcal{E}})$, coordinate $(\theta - \theta_{\mathcal{E}})$, mass mr^2, and spring constant k_θ given by

$$k_\theta = \left[\frac{d^2V(\theta)}{d\theta^2}\right]_{\theta_c} = \left(\frac{d^2V(\theta)}{d\theta^2}\right)_{\theta_c} + \frac{(\sin^2\theta_c + 3\cos^2\theta_c)}{\sin\theta_c\cos\theta_c}\left(\frac{dV(\theta)}{d\theta}\right)_{\theta_c} \quad (37)$$

The motion of the geocentric right ascension in the undisturbed mode is given by,

$$\dot{\phi}_\theta^2 = \frac{1}{mr^2\sin\theta_c\cos\theta_c}\left(\frac{dV(\theta)}{d\theta}\right)_{\theta_c} \quad (38)$$

while after the impulse is applied, the colatitude angular component of the radius vector oscillates about the equilibrium value θ_c with a frequency given by

$$\omega_\theta^2 = \frac{k_\theta}{mr^2} = \left[\frac{1}{mr^2}\left(\frac{d^2V(\theta)}{d\theta^2}\right)_{\theta_c} + \frac{1}{mr^2}\frac{(\sin^2\theta_c + 3\cos^2\theta_c)}{\sin\theta_c\cos\theta_c}\left(\frac{dV(\theta)}{d\theta}\right)_{\theta_c}\right] \quad (39)$$

The relationships between ω_θ and $\dot{\phi}_\theta$ is,

$$\omega_\theta = \left\{\left[\frac{1}{mr^2}\left(\frac{d^2V(\theta)}{d\theta^2}\right)_{\theta_c} + \frac{1}{mr^2}\frac{(\sin^2\theta_c + 3\cos^2\theta_c)}{\sin\theta_c\cos\theta_c}\left(\frac{dV(\theta)}{d\theta}\right)_{\theta_c}\right] mr^2\sin\theta_c\cos\theta_c \times \left/\left(\frac{dV(\theta)}{d\theta}\right)_{\theta_c}\right\}^{1/2}\dot{\phi}_\theta. \quad (40)$$

Here, the frequency of the angular component is also given in terms of the equilibrium value of the orbital period, and the first two derivatives of the potential energy, but with respect to the colatitude.

At this point, it is instructive to choose some representations for the gravitational potential given by (23) and calculate ω_r and ω_θ for each case.

Case I. Let us assume that the Earth is perfectly spherical, and homogeneous in density. The potential is then given by

$$V = \frac{\mu}{r} \tag{41}$$

Here then,

$$\frac{dV(r)}{dr} = \frac{-\mu}{r_{\mathcal{E}}},$$

and

$$\frac{d^2V(r)}{dr^2} = \frac{2\mu}{r_{\mathcal{E}}^3},$$

and from equations (31) and (25),

$$k_{r(\mu)} = \frac{2\mu}{r_{\mathcal{E}}^3} + 3m \sin^2\theta \dot{\phi}^2. \tag{42}$$

From (29),

$$\dot{\phi}^2_{r(\mu)} = \frac{-\mu}{mr_{\mathcal{E}}^3 \sin^2\theta}, \tag{43}$$

which yields,

$$k_{r(\mu)} = \frac{-\mu}{r_{\mathcal{E}}^3}, \tag{44}$$

and

$$\omega^2_{r(\mu)} = \frac{k}{m} = \frac{-\mu}{mr_{\mathcal{E}}^3}, \tag{45}$$

in which case,

$$\frac{\dot{\phi}^2_{r(\mu)}}{\omega^2_{r(\mu)}} = \frac{1}{\sin^2 \theta} \tag{46}$$

or,

$$\omega_{r(\mu)} = \sin \theta \dot{\phi}_{r(\mu)} \tag{47}$$

Since $dV(r)/d\theta = 0$ for the central force potential, then $\omega_\theta(\mu) = 0$. Equation (47) is an oscillation in r superposed upon a motion around the z-axis with an angular velocity given by equation (29); $\dot{\phi}_{r(\mu)}$ will vary slightly as r oscillates, but will remain very nearly equal to the constant value given by equation (43). If our reference frame is rotated so that the z-axis is always perpendicular to the orbital plane, then $\sin \theta = 1$, and equation (47) reduces to

$$\omega_{r(\mu)} = \dot{\phi}_{r(\mu)}. \tag{48}$$

For the case of the spherical Earth, the radial component of the perturbed radius vector has the same period of oscillation or rotation as that of the orbit, and will execute one oscillation per revolution of orbit.

Case II. Let us now consider the case where the Earth is represented as a perfect rotational ellipsoid, and its potential is given by

$$V = \frac{\mu}{r}\left[1 + \frac{J_2}{2}\left(\frac{r_e}{r}\right)^2 (3\cos^2 \theta - 1)\right]. \tag{49}$$

Proceeding as in the above case we have for the radial component,

$$\dot{\varphi}^2_{r(\mu+J_2)} = \frac{-\mu}{mr_\mathcal{E}^3 \sin^2\theta}\left[1 + \frac{3}{2}\left(\frac{r_e}{r_\mathcal{E}}\right)^2 J_2(3\cos^2\theta - 1)\right], \tag{50}$$

$$\omega^2_{r(\mu+J_2)} = \frac{k_r}{m} = \frac{-\mu}{mr_\mathcal{E}^2}\left[1 - \frac{3}{2}\left(\frac{r_e}{r_\mathcal{E}}\right)^2 J_2(3\cos^2\theta - 1)\right], \tag{51}$$

and

$$\omega_{r(\mu+J_2)} = \sin\theta\left\{\frac{1 - \left(\frac{3J_2 r_e^2}{2r_\mathcal{E}^2}\right)(3\cos^2\theta - 1)}{1 + \left(\frac{3J_2 r_e^2}{2r_\mathcal{E}^2}\right)(3\cos^2\theta - 1)}\right\}^{1/2} \dot{\phi}_{r(\mu+J_2)}. \tag{52}$$

For the θ component,

$$\dot{\phi}^2_{\theta(\mu+J_2)} = \frac{3\mu J_2}{mr^3}\left(\frac{r_e}{r}\right)^2, \tag{53}$$

$$\omega^2_{\theta(\mu+J_2)} = \frac{k_\theta}{mr^2} = \frac{3\mu J_2}{mr^3}\left(\frac{r_e}{r}\right)^2 \cos^2\theta_\mathcal{E}, \tag{54}$$

and

$$\omega_{\theta(\mu+J_2)} = \cos\theta_\mathcal{E}\dot{\phi}_{\theta(\mu+J_2)}. \tag{55}$$

Equations (52) and (55) are again referenced to our original fixed inertial z-axis. By rotating the coordinate system so as to make the z-axis lie perpendicular to the orbital plane, we again have that sin θ = 1, and cos θ = 0, in equation (52), while a rotation of x-coincidental with the radius vector wil' make cos $\theta_\mathcal{E}$ = 1 in

equations (55). A transformation of these quantities into the planes of motion of the tracking errors are necessary to describe the oscillatory behavior of the latter in terms of ω_r and ω_θ. The fact that $\omega_{\theta(\mu)} = 0$, for the spherical Earth results of course, from the fact that we have in that case only central force motion. As a result, if a small impulse were applied normal to the plane of motion, the effect would be only to change slightly, the inclination of the orbit. It would however, remain fixed at the new inclination. There would be no oscillatory motion in θ. The second case, namely that of an Earth's gravitational potential containing a zeroth, and second zonal harmonic only is somewhat more interesting. Equation (55) where $\cos \theta_{\mathcal{E}} = 1$, indicates that the θ -component executes one full cycle per revolution of the orbit, similar to the radial component given by equation (47). After rotation, equation (52) reduces to,

$$\omega_{r(\mu+J_2)} = \left\{ \frac{1 - \frac{3|J_2|}{2}\left(\frac{r_e}{r_{\mathcal{E}}}\right)^2}{1 + \frac{3|J_2|}{2}\left(\frac{r_e}{r_{\mathcal{E}}}\right)^2} \right\}^{1/2} \dot{\phi}_{r(\mu+J_2)}. \qquad (56)$$

Here, we have included the sign of J_2, the coefficient of the Earth's second zonal harmonic. Since the magnitude of J_2 is approximately 0.10825×10^{-2}, then the coefficient of $\dot{\phi}_{r(\mu+J_2)}$ is only slightly less than unity. This means that the frequency of oscillation of the radial component of the perturbed radius vector is also slightly less than the rotational frequency of the spacecraft in its orbit.

From this then, the period of revolution of the radial component given by $P_{\omega_r} = 2\pi/\omega_r$, will be larger than the natural period of the orbit, $P_{\dot{\phi}_r} = 2\pi/\dot{\phi}_r$. This frequency shift, and correponding change in period is induced by the inclusion of the J_2 term or second zonal harmonic in the Earth's potential. As a result, the mass redistribution is equivalent to a change in the spring constant of a translational mechanical circuit or the capacitance of the electrical series circuit. In this case, our results are now written,

$$\omega_{r(\mu+J_2)} = \left\{ \frac{1 - \frac{3|J_2|}{2}\left(\frac{r_e}{r_\mathcal{E}}\right)^2}{1 + \frac{3|J_2|}{2}\left(\frac{r_e}{r_\mathcal{E}}\right)^2} \right\}^{1/2} \dot{\phi}_{r(\mu+J_2)}, \tag{57}$$

and

$$\omega_{\theta(\mu+J_2)} = \dot{\phi}_{\theta(\mu+J_2)}. \tag{58}$$

In words, if a small but finite impulse is applied to an Earth satellite in orbit about an Earth described by a perfect rotational ellipsoid, the radial component of the radius vector will oscillate about its equilibrium value with a frequency whose value is

$$\left\{ \frac{1 - \frac{3|J_2|}{2}\left(\frac{r_e}{r_\mathcal{E}}\right)^2}{1 + \frac{3|J_2|}{2}\left(\frac{r_e}{r_\mathcal{E}}\right)^2} \right\}^{1/2}$$

times that of the geocentric right ascension. The frequency in θ is identical to that of the geocentric right ascension. Also, the indication here is that we should expect a shift in both the frequency of the radial and cross-track errors, as either the number of, or the values of the coefficients of the gravitational potential terms is changed. To show that this may be true also for the angular component we list the results of calculations for an Earth whose potential includes the zeroth, second and third zonal harmonics, and finally, the zeroth, second, third and fourth zonal harmonics.

Case III.

$$V = \frac{\mu}{r}\left[1 + \frac{J_2}{2}\left(\frac{r_e}{r}\right)^2 (3\cos^2\theta - 1) + \frac{J_3}{2}\left(\frac{r_e}{r}\right)^3 (5\cos^3\theta - 3\cos\theta)\right] \tag{59}$$

Here,

$$\dot{\phi}^2_{r(\mu+J_2+J_3)} = \frac{-\mu}{mr_\mathcal{E}^3 \sin^2\theta}\left\{1 - \frac{1}{2}\left(\frac{r_e}{r_\mathcal{E}}\right)^2\left[3J_2(3\cos^2\theta - 1) + 20\,J_3\left(\frac{r_e}{r_\mathcal{E}}\right)\right.\right.$$

$$\left.\left. \times \left(\cos^3\theta - \frac{3}{5}\cos\theta\right)\right]\right\}, \tag{60}$$

$$\omega^2_{r(\mu+J_2+J_3)} = \frac{-\mu}{mr_\mathcal{E}^3}\left\{1 + \frac{1}{2}\left(\frac{r_e}{r_\mathcal{E}}\right)^2\left[3J_2(3\cos^2 - 1) + 20J_3\left(\frac{r_e}{r_\mathcal{E}}\right)\left(\cos^3\theta - \frac{3}{5}\cos\theta\right)\right]\right\}$$

(61)

and

$$\omega_{r(\mu+J_2+J_3)} = \sin\theta \left\{ \frac{1 + \frac{1}{2}\left(\frac{r_e}{r_\varepsilon}\right)^2 \left[3J_2(3\cos^2\theta - 1) + 20J_3\left(\frac{r_e}{r_\varepsilon}\right)\left(\cos^3\theta - \frac{3}{5}\cos\theta\right)\right]}{1 - \frac{1}{2}\left(\frac{r_e}{r_\varepsilon}\right)^2 \left[3J_2(3\cos^2\theta - 1) + 20J_3\left(\frac{r_e}{r_\varepsilon}\right)\left(\cos^3\theta - \frac{3}{5}\cos\theta\right)\right]} \right\}^{1/2}$$

$$\times \dot{\phi}_{r(\mu+J_2+J_3)}. \tag{62}$$

Also,

$$\dot{\phi}^2_{\theta(\mu+J_2+J_3)} = \frac{3\mu}{2mr^3}\left(\frac{r_e}{r}\right)^2 \left[2J_2 + J_3\left(\frac{r_e}{r}\right)\left(5\cos\theta_\varepsilon - \frac{1}{\cos\theta_\varepsilon}\right)\right]. \tag{63}$$

$$\omega^2_{\theta(\mu+J_2+J_3)} = \frac{3\mu}{2r}\left(\frac{r_e}{r}\right)^2 \left[2J_2\cos^2\theta_\varepsilon + J_3\left(\frac{r_e}{r}\right)\left(25\cos^3\theta_\varepsilon - 8\cos\theta_\varepsilon - \frac{1}{\cos\theta_\varepsilon}\right)\right] \tag{64}$$

and

$$\omega_{\theta(\mu+J_2+J_3)} = \cos\theta \left\{ \frac{2J_2 + J_3\left(\frac{r_e}{r}\right)\left(25\cos\theta_\varepsilon - \frac{8}{\cos\theta_\varepsilon} - \frac{1}{\cos^3\theta_\varepsilon}\right)}{2J_2 + J_3\left(\frac{r_e}{r}\right)\left(5\cos\theta_\varepsilon - \frac{1}{\cos\theta_\varepsilon}\right)} \right\}^{1/2} \phi_{\theta(\mu+J_2+J_3)} \tag{65}$$

Case IV.

$$V = \frac{\mu}{r}\left[1 + \frac{J_2}{2}\left(\frac{r_e}{r}\right)^2 (3\cos^2\theta - 1) + \frac{5}{2}J_3\left(\frac{r_e}{r}\right)^3 \left(\cos^3\theta - \frac{3}{5}\cos\theta\right)\right.$$

$$\left. + \frac{1}{8}J_4\left(\frac{r_e}{r}\right)^4 (35\cos^4\theta - 30\cos^2\theta + 3)\right] \tag{66}$$

$$\dot{\phi}_{(\mu+J_2+J_3+J_4)} = \frac{-\mu}{mr_\mathcal{E}^3 \sin^2\theta}\left[1 - \frac{5}{2}J_2\left(\frac{r_e}{r_\mathcal{E}}\right)^2 (3\cos^2\theta - 1)\right.$$

$$- 10\,J_3\left(\frac{r_e}{r_\mathcal{E}}\right)^3 \left(\cos^3\theta - \frac{3}{5}\cos\theta\right)$$

$$\left. - \frac{5}{8}J_4\left(\frac{r_e}{r_\mathcal{E}}\right)^4 (35\cos^4\theta - 30\cos^2\theta + 3)\right], \qquad (67)$$

$$\omega^2_{r(\mu+J_2+J_3+J_4)} = \frac{-\mu}{mr^3}\left[1 + \frac{3}{2}J_2\left(\frac{r_e}{r_\mathcal{E}}\right)^2 (3\cos^2\theta - 1)\right.$$

$$+ 10\,J_3\left(\frac{r_e}{r_\mathcal{E}}\right)^3 \left(\cos^3\theta - \frac{3}{5}\cos\theta\right)$$

$$\left. + \frac{5}{8}J_4\left(\frac{r_e}{r_\mathcal{E}}\right)^4 (35\cos^4\theta - 30\cos^2\theta + 3)\right], \qquad (68)$$

$$\omega_{r(\mu+J_2+J_3+J_4)} = \sin\theta \left\{ \frac{1 + \frac{3}{2}J_2\left(\frac{r_e}{r_\mathcal{E}}\right)^2 (3\cos^2\theta - 1) + 10\,J_3\left(\frac{r_e}{r_\mathcal{E}}\right)^3 \left(\cos^3\theta - \frac{3}{5}\cos\right.}{1 - \frac{3}{2}J_2\left(\frac{r_e}{r_\mathcal{E}}\right)^2 (3\cos^2\theta - 1) - 10\,J_3\left(\frac{r_e}{r_\mathcal{E}}\right)^3 \left(\cos^3\theta - \frac{3}{5}\cos\theta\right)} \right.$$

$$\left. \frac{+ \frac{5}{8}J_4\left(\frac{r_e}{r_\mathcal{E}}\right)^4 (35\cos^4\theta - 30\cos^2\theta + 3)}{- \frac{5}{8}J_4\left(\frac{r_e}{r_\mathcal{E}}\right)^4 (35\cos^4\theta - 30\cos^2\theta + 3)} \right\}^{1/2} \phi_{r(\mu+J_2+J_3+J_4)}, \qquad (69)$$

and,

$$\dot{\phi}^2_{\theta(\mu+J_2+J_3+J_4)} = \frac{3\mu}{2mr^3}\left(\frac{r_e}{r}\right)^2\left[2J_2 + J_3\left(\frac{r_e}{r}\right)\left(5\cos\theta_{\mathcal{E}} - \frac{1}{\cos\theta_{\mathcal{E}}}\right)\right.$$

$$\left. + \frac{J_4}{8}\left(\frac{r_e}{r}\right)^2 (140\cos^2\theta_{\mathcal{E}} - 60)\right], \tag{70}$$

$$\omega^2_{\theta(\mu+J_2+J_3+J_4)} = \frac{3\mu\cos^2\theta_{\mathcal{E}}}{2mr^3}\left(\frac{r_e}{r}\right)^2\left[2J_2 + J_3\left(\frac{r_e}{r}\right)\left(25\cos\theta_{\mathcal{E}} - \frac{8}{\cos\theta_{\mathcal{E}}} - \frac{1}{\cos^3\theta_{\mathcal{E}}}\right)\right.$$

$$\left. + \frac{J_4}{8}\left(\frac{r_e}{r}\right)^2 (140\cos^2\theta_{\mathcal{E}} - 60)\right]. \tag{71}$$

with

$$\omega_{\theta(\mu+J_2+J_3+J_4)} = \cos\theta_{\mathcal{E}}\left\{\frac{2J_2 + J_3\left(\frac{r_e}{r}\right)\left(25\cos\theta_{\mathcal{E}} - \frac{8}{\cos\theta_{\mathcal{E}}} - \frac{1}{\cos^3\theta_{\mathcal{E}}}\right)}{2J_2 + J_3\left(\frac{r_e}{r}\right)\left(5\cos\theta_{\mathcal{E}} - \frac{1}{\cos\theta_{\mathcal{E}}}\right)}\right.$$

$$\left.\frac{+\frac{J_4}{8}\left(\frac{r_e}{r}\right)^2 (140\cos^2\theta_{\mathcal{E}} - 60)}{+\frac{J_4}{8}\left(\frac{r_e}{r}\right)^2 (140\cos^2\theta_{\mathcal{E}} - 60)}\right\}^{1/2} \dot{\phi}_{\theta(\mu+J_2+J_3+J_4)} \tag{72}$$

From the gereral equations (35) and (40, one can obtain $\dot{\phi}_r/\omega_r$ and $\dot{\phi}_\theta/\omega_\theta$ for any number of zonal harmonics. It is of interest to compare the coefficients of μ, or the brackett terms of $\dot{\phi}^2_r$ and ω^2_r with the expression for the anomalistic mean motion,

$$\overline{n} = n_0 \left[1 + \frac{3}{2} J_2 \frac{r_e^2 \sqrt{1 - e^2}}{a(1 - e^2)} \left(1 - \frac{3}{2} \cos^2 \theta\right)\right], \tag{73}$$

where $n_0 = (\mu/a^3)^{1/2}$ for central force motion, a is the semi-major axis, and e is the eccentricity. The right hand side is expanded through the coefficient of the second zonal harmonic only, and can be compared to equations (50) and (51) for $\dot{\phi}_r^2$ and ω_r^2.

V. TIME AVERAGES

Figures 6(a) and (b) are pictorial representations of translational mechanical and series electrical circuits. The general differential equations for these systems are

$$\text{(a)} \quad \frac{Md^2y}{dt^2} + \nu \frac{dy}{dt} + ky = F_0 \cos \omega t, \quad \text{translational mechanical.}$$

$$\text{(b)} \quad \frac{Ld^2i}{dt^2} + R \frac{di}{dt} + \frac{i}{c} = -\omega E_0 \sin \omega t, \text{ series electrical.} \tag{74}$$

The vertical displacement coordinate of the weight is y, M is the vibrating mass, ν is the friction, k, the spring constant, F_0 and ω_F, the amplitude and frequency of the impressed driving force, respectively. For the electrical case, L is the inductance, c, the capacitance, R, the resistance, E_0 and ω_E the amplitude and frequency of the impressed voltage, and i, the current coordinate flowing around the loop. If ν (R) is zero, then the system is a conservative one. If no driving forces are present, then the equations are homogeneous, and the natural or resonant frequencies are given by

$$\omega_n = \sqrt{\frac{k}{M}}, \quad \text{and} \quad \frac{1}{\sqrt{LC}}. \tag{75}$$

The frequency be made to vary by changing the equivalent mass or spring constant of the system. In our problem, the mass is constant but the restoring force will depend upon the number of harmonics in the potential, or in other words, the distribution of the Earth's mass. From our results above, if we take J_2 to be approximately $J_2 = -1.0825 \times 10^{-3}$, $J_3 = 2.5450 \times 10^{-6}$, and $J_4 = 1.6715 \times 10^{-6}$ where $\mu = 1$, then the effect of including the third and fourth zonal harmonics is to shift the value of ω_r and ω_θ, opposite to that of J_2. However, since J_2 is of the order of 10^3 times J_3 or J_4, the latter effect is very small. In any event, equations (35) and (40) predict a phase shift due to uncertainties and variations in the terms of the gravitational potential. The amplitude of the oscillation for a free, conservative system, representing a solution of equations of the type (74) is given by

$$N = N_0 \cos(\omega_\theta t + \delta_\theta), \tag{76}$$

for the cross-track error, and

$$R = R_0 \cos(\omega_r t + \delta_r), \tag{77}$$

for the radial uncertainty. Here N_0 and R_0 are the maximum error amplitudes for each case, and δ is a corresponding phase angle. Since the epoch times are taken to be the same for both observed and computed data, then the phase angle is set equal to zero. Let us now examine the time averages of the cross and

radial uncertainties. The time averages of equations (76) and (77) are obtained by integrating both sides with respect to t from 0 to τ, and dividing by τ:

$$\frac{1}{\tau}\int_0^{\tau} N dt = \frac{1}{\tau}\int_0^{\tau} N_0 \cos \omega_\theta t dt = \frac{1}{\tau}\frac{N_0}{\omega_\theta}[\cos(\omega_\theta \tau) - 1] \tag{78}$$

Since N_0 and ω_θ are constant, when $\omega_\theta \tau = 2n\pi$, where n = 0, 1, 2, . . . , then,

$$\frac{1}{\tau}\int_0^{\tau} N dt = 0. \tag{79}$$

That is, if τ is chosen to be the period, then (78) vanishes. Even if $\omega_\theta \tau$ is not an integer multiple of 2π, the maximum value that the bracket portion of (78) can be is 1, but choosing τ sufficiently long, the right hand side of (78) can be made as small as desired. In this case,

$$\bar{N} = \frac{1}{\tau \to \infty}\int_0^{\tau} N dt \to 0 \tag{80}$$

Similarly,

$$\bar{R} = \frac{1}{\tau \to \infty}\int_0^{\tau} R dt \to 0 \tag{81}$$

VI. CONCLUSIONS

In section III, we obtained relationships between the behavior of the radial and cross track errors and uncertainties in the orbital elements. In section IV, we found the equations relating this behavior to certain terms of the Earth's gravitational field. An examination of figures 2, 3, 4, and 5, indicates that the tracking errors oscillate harmonically with a frequency close to that of the orbital frequency. The wave interference analysis shows that the radial frequency is one half the sum of the observed and computed orbital frequencies. These frequencies are functions of the semimajor axis of the orbit. The analysis of section IV shows that except for the case of a spherical Earth, the radial frequency is a function of the gravitational potential energy and the orbital frequency. Both results are consistent in that they show a proper frequency or phase shift for the radial oscillation. Results for the cross track case are similar, except that this phase shift does not appear until the computation potential includes the third zonal harmonic or higher. This indicates that quantitatively, there appears to be a lack of uncertainty in the eccentric anomaly and argument of perigee for the spherical Earth case, which is reasonable, since the orbit is then bound and closed and completely determined with full accuracy for all time.

From these considerations, there emerges the following physical picture for the tracking error problem: The Earth-satellite system and the corresponding orbit differences are considered as a harmonic oscillator system whose frequency is determined by the ratio of the spring constant to the mass for the

case of a translational mechanical system, or by the inverse product of the inductance (inertia) times the capacitance (elastance) for an electrical series circuit. In our case, the spring constants or capacitances are described in terms of the first and second spatial derivatives of the Earth's potential. The gravitational potential, which as a solution of Laplace's equation, involves here, only the ordinary Legendre polynomials, and these in turn, are determined by the distribution of mass in the Earth. This distribution therefore is described by the assigned values of the coefficients of these zonal harmonics.

The results we have obtained in this paper are valid for conservative systems, namely those in which the total energy and angular momentum are conserved. The frequency equations that we developed in section IV, assume an azimuthally symmetric potential. Because of this, the corresponding canonical momentum is a constant of the motion, and this led us to our analytic expressions for the tracking frequencies as functions of the potential. An important technique in theoretical physics is to look for symmetries within the system. For each symmetry, there follows a conservation law, which simplifies calculation of physical properties of the system. This approach, combined with the method of solution by separable Hamiltonian, makes it possible to do the gravitational theory of a satellite orbit very accurately, and without the use of perturbation theory (References 5, 6). In addition, a method has been developed (Reference 7) which permits separation of the Hamilton Jacobi equation in the presence of a nonconservative force such as air drag. In this case, the atmospheric density

is incorporated into the equations of motion in an analytic fashion by fitting an exponential form to an accurate density profile. This allows one to integrate the variational equations of the orbital elements due to air drag in terms of elementary functions. This then has the effect of advancing the boundary conditions on the Hamilton-Jacobi equation. As a result, it is possible to include atmospheric resistance in orbital error analysis.

It is expected that the results obtained here especially those of sections III and IV, are to be extended in forthcoming analyses to more detailed cases such as given in figures 4 and 5, for GEOS-II.

ACKNOWLEDGMENTS

The authors would like to express their gratitude to Mr. John Foreman of the Computer Sciences – Technicolor Associates, Seabrook, Maryland and to Mr. William Muse of the Thiokol Corporation, Ogden, Utah, for their valuable discussions on this subject matter, and their assistance with many calculations.

REFERENCES

1. Bonavito, N. L., and Watson, J. S., "Dynamical Error Analysis In Orbit Determination Systems," Goddard X-550-71-20, January, 1971.

2. Brouwer, D., "Solution of the Problem of Artificial Satellite Theory Without Drag," Astron. J. 64(9):378-397, November, 1959.

3. Lerch, F. J., "Gravitational Field Models for the Earth," Goddard X-553-72-146, May, 1972.

4. Gaposchkin, E. M., Lambeck, K., "1969, Smithsonian Standard Earth (II)," SAO Special Report 315, May, 1970.

5. Vinti, J. P., "Inclusion of the Third Zonal Harmonic in an Accurat eference Orbit of an Artificial Satellite," J. Res., Nat. Bur. Std. (U.S.), 70B, No. 1, January-March, 1966.

6. Bonavito, N. L., "Computational Procedure for Vinti's Accurate Reference Orbit with Inclusion of the Third Zonal Harmonic," NASA TN D-3562, August, 1966.

7. Watson, J. S., Mistretta, G. D., and Bonavito, N. L., "An Analytic Method to Account for Drag In the Vinti Satellite Theory," Goddard X-932-74-99, April, 1974. Also, "Journal of Celestial Mechanics, 11, 1975.

FIGURE CAPTIONS

Figure 1. Two waves of nearly equal frequency (a) and with equal magnitudes, (b) are differenced, (c) to give a wave whose amplitude (dashed line) varies periodically. The effect described from (b) to (c) is commonly referred to as the phenomenon of beats.

Figure 2(a). Short term view of the radial error for the Cannonball satellite.

Figure 2(b). Expanded time scale for the radial error of the Cannonball satellite.

Figure 3. Expanded time scale of the cross track error for the Cannonball satellite.

Figure 4. Tracking errors for the GEOS-II satellite using GEM 1 (doppler data).

Figure 5. Tracking errors for the GEOS-II satellite using 69 SAO Standard Earth (doppler data).

Figure 6. Physical systems whose natural frequencies are equivalent to tracking error oscillations.

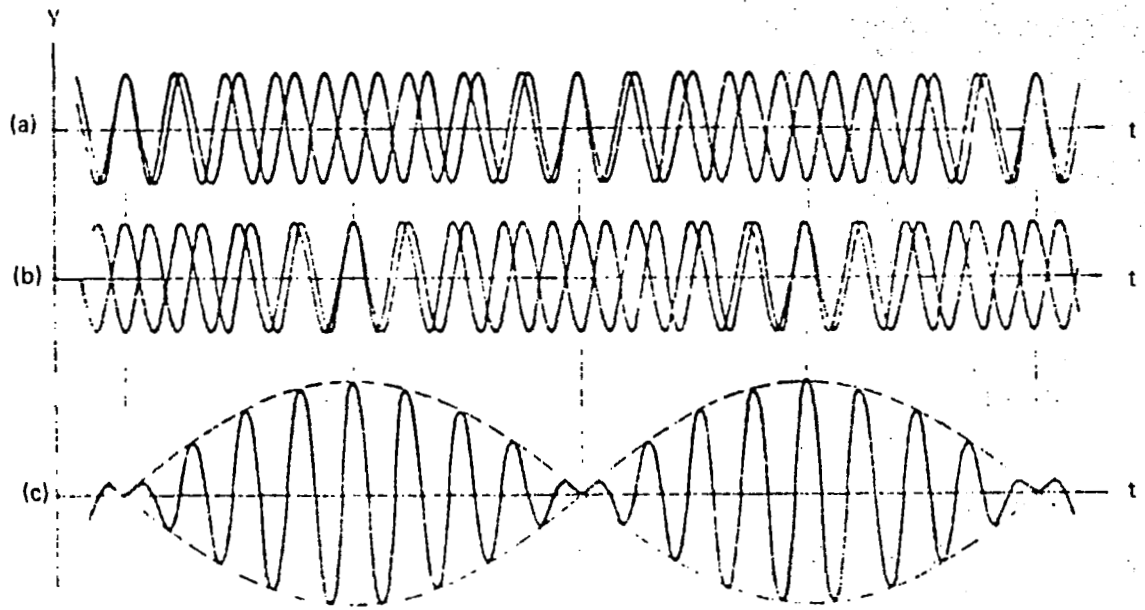

Figure 1. Two waves of nearly equal frequency (a) and with equal magnitudes, (b) are differenced, (c) to give a wave whose amplitude (dashed line) varies periodically. The effect described from (b) to (c) is commonly referred to as the phenomenon of beats.

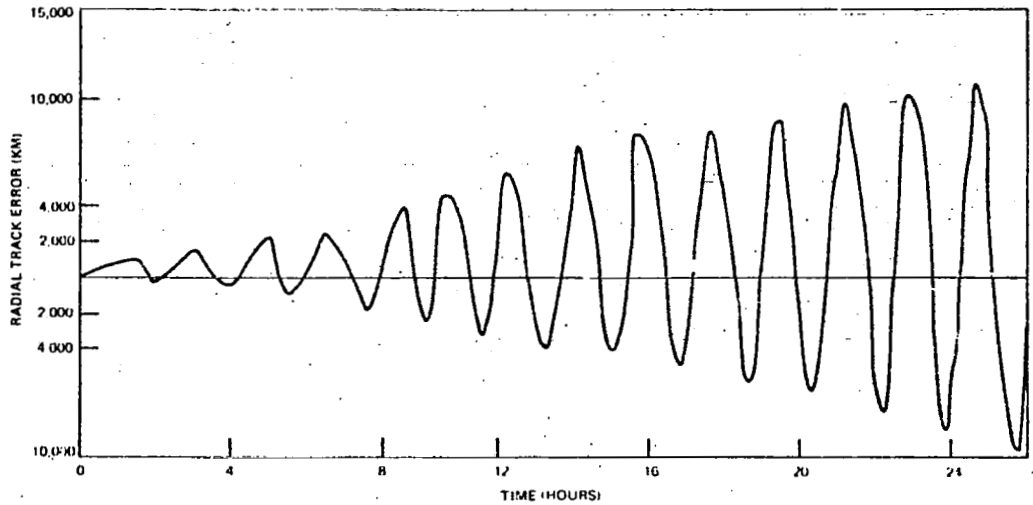

Figure 2(a). Short term view of the radial error for the Cannonball satellite

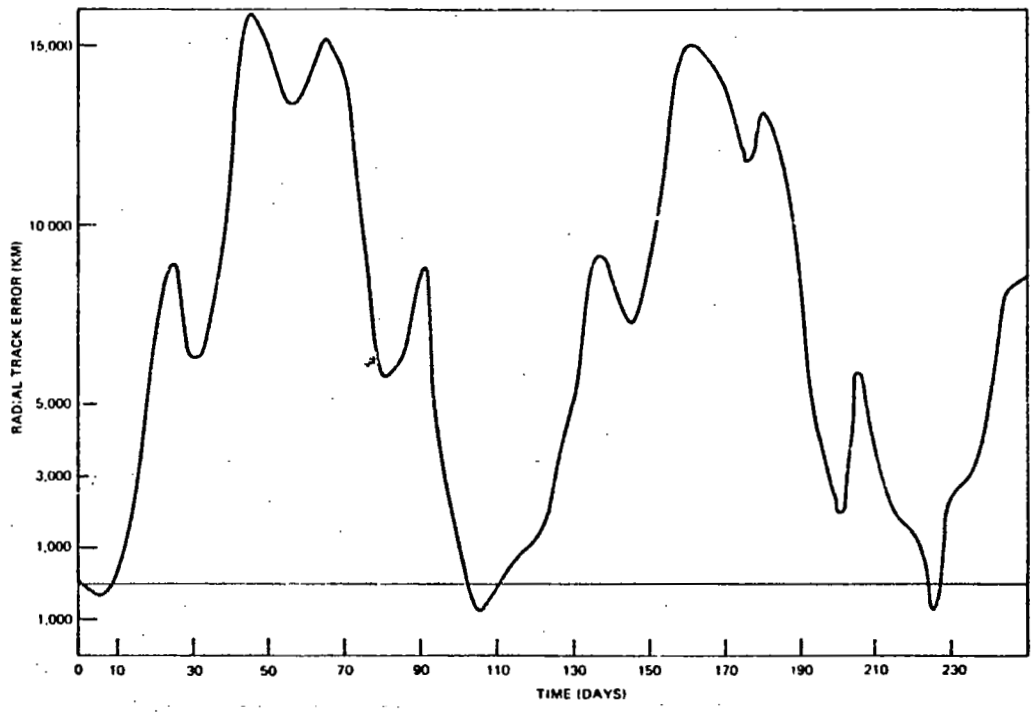

Figure 2(b). Expanded time scale for the radial error of the Cannonball satellite

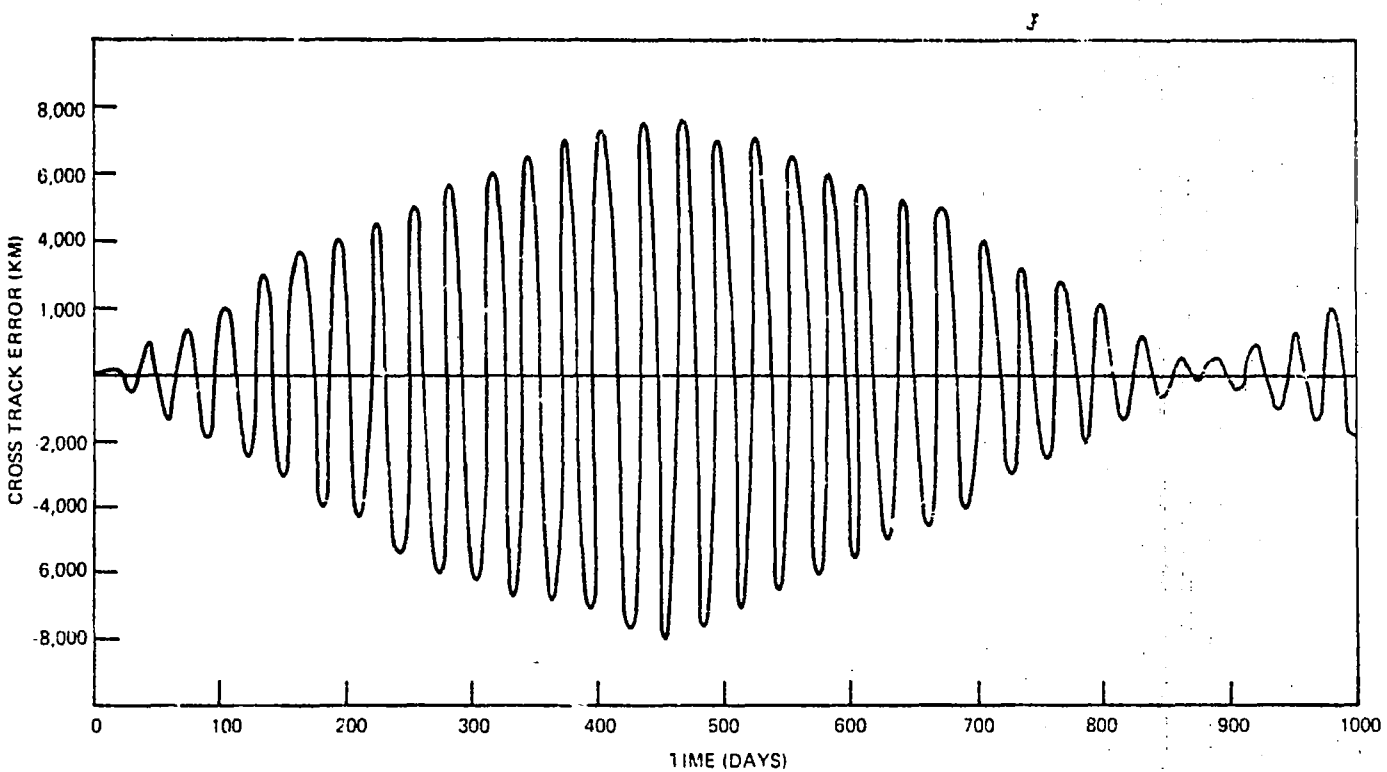

Figure 3. Expanded time scale of the cross track error for the Cannonball satellite

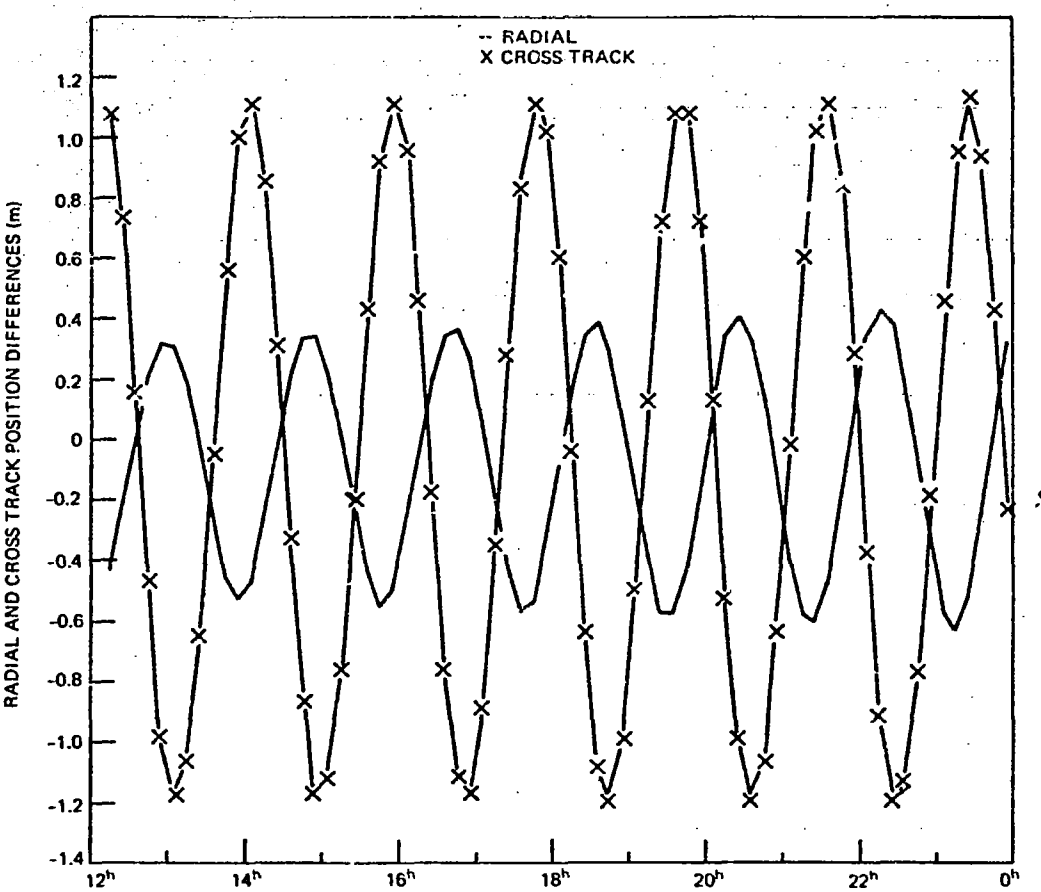

Figure 4. Tracking errors for the GEOS-II satellite using GEM 1 (doppler data)

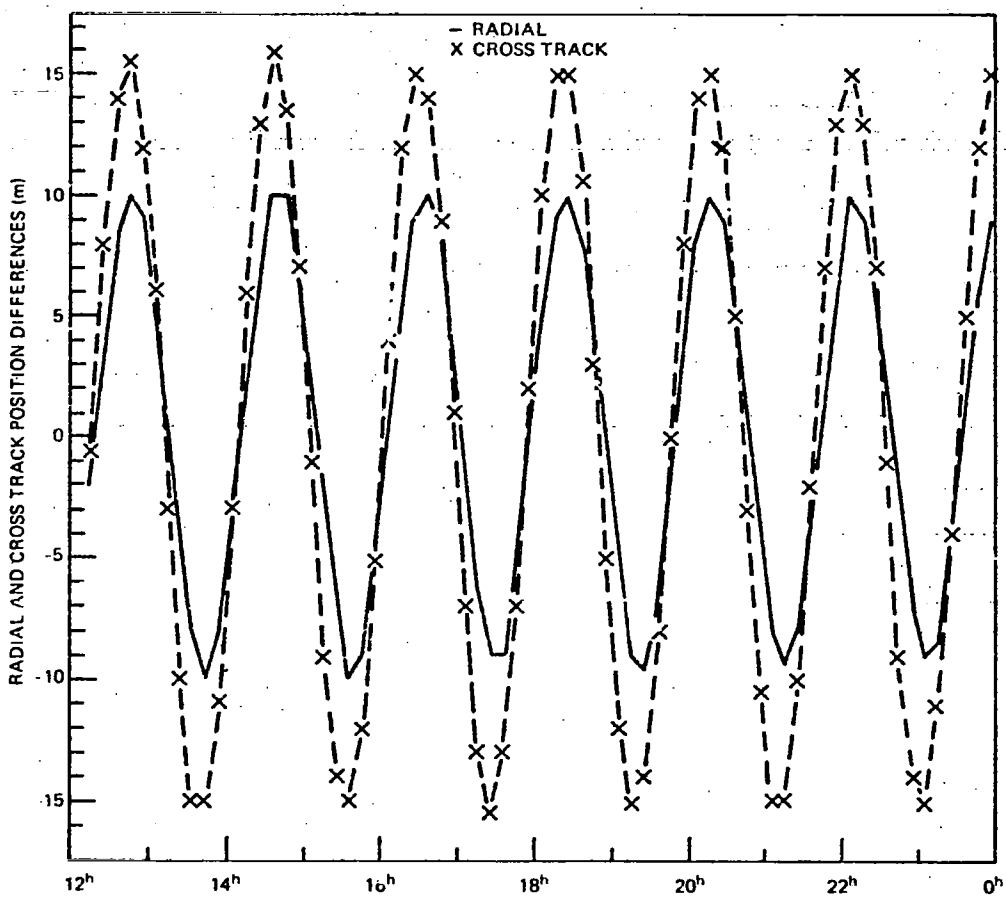

Figure 5. Tracking errors for the GEOS-II satellite using 69 SAO Standard Earth (doppler data)

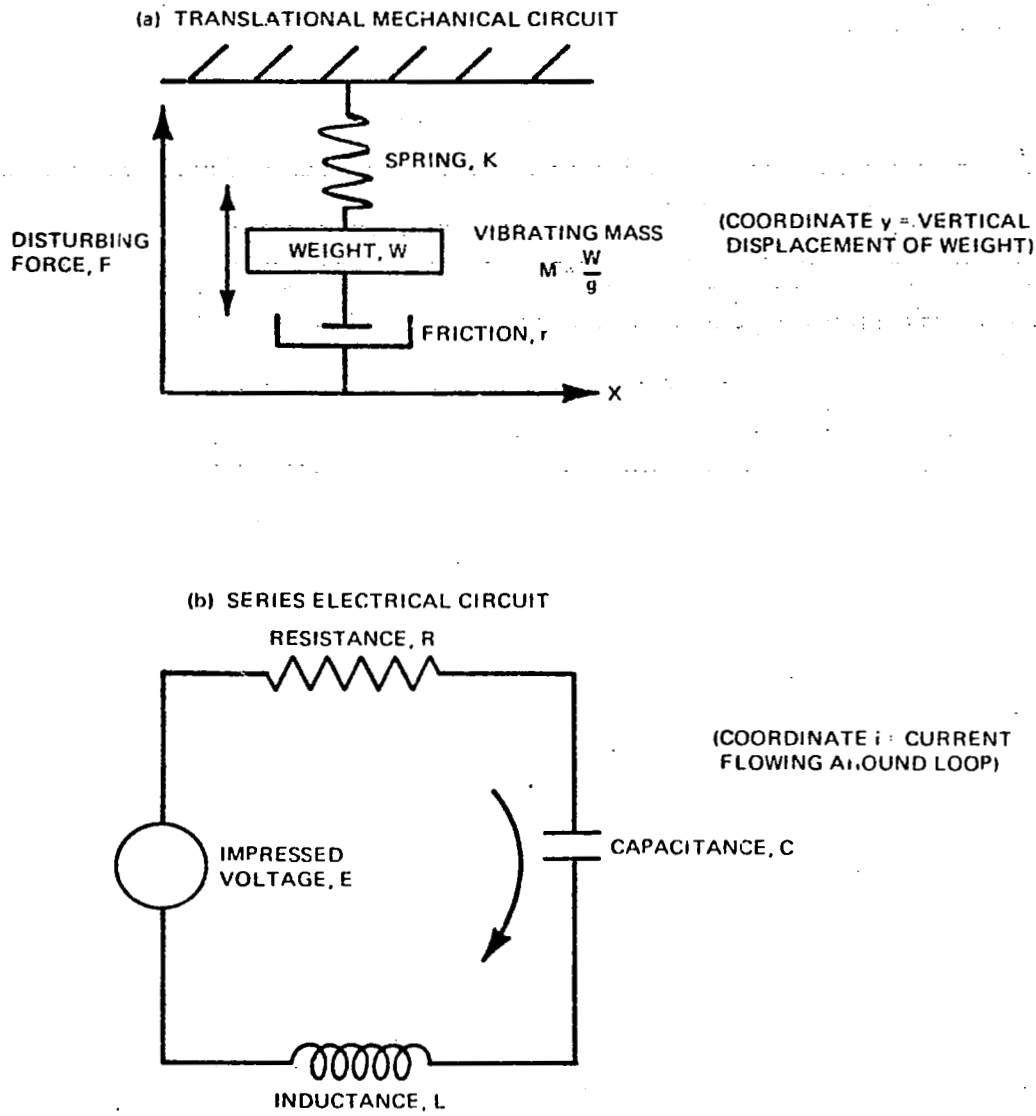

Figure 6. Physical systems whose natural frequencies are equivalent to tracking error oscillations

END

DATE

FILMED

JUN 3 1975